Effects of Hydrophobic Interaction on Rheological Behavior and Microstructure of Carboxylated Core-Shell Latex Suspension

Hiroshi Nakamura, Kazuyuki Tachi

Toyota Central Research & Development Laboratories, Inc., 41–1, Yokomichi, Nagakute, Aichi-gun, Aichi, 480-1192, Japan

Received 1 June 2005; accepted 25 October 2005
DOI 10.1002/app.23536
Published online in Wiley InterScience (www.interscience.wiley.com).

ABSTRACT: We have investigated the effects of hydrophobic interactions on the rheological behavior and microstructure of suspension of carboxylated core-shell latex particles with changing hydrophobicity of shell polymer and suspending medium. The carboxylated core-shell latex particles formed lattice-like microstructures in aqueous suspension with dissociation of carboxyl groups. With increasing hydrophobicity of the shell polymer, the interparticle distance ξ in the microstructure decreased. However, ξ increased with increasing hydrophobicity of the suspending medium. The effect of hydrophobic interaction on ξ was explained by the steric stabilization theory for particles with grafted polymer on the surface. As the carboxylated core-shell latex particles overlapped each other in the microstructure, an attractive force was generated between the particles in aqueous suspension. With increasing hydrophobicity of the shell, the attractive force increased, but with increasing hydrophobicity of the suspending medium, the attractive force decreased. © 2006 Wiley Periodicals, Inc. J Appl Polym Sci 101: 4153–4158, 2006

Key words: viscoelastic properties; viscosity; shear; rheology; core-shell polymers

INTRODUCTION

Core-shell structured latex particles consisting of a core polymer and a shell polymer containing carboxyl groups swell with addition of base in aqueous medium.[1–3] An aqueous suspension of the swelled particles displays shear-thinning flow at relatively low concentrations, in spite of indicating Newtonian flow with nonswelling particles.[4–9] We found that swelling of particles was dominated by electrical repulsion between carboxyl ions and hydrophobic attraction between hydrophobic groups in shell polymers.[1]

In our previous works, it was found from dynamic oscillatory rheological measurements and small angle X-ray scattering measurements[10] that the shear-thinning flow suspensions of the core-shell structured carboxylated latex particle had lattice-like microstructures. The microstructure was formed and deformed by thermal motion of the particles.[10] It could be assumed that the lattice-like microstructure was formed by attractive and repulsive forces between the core-shell particles. The repulsive force must have been generated by steric interactions between shell polymers and electrostatic interactions between carboxyl ion groups of shell polymers, i.e., electrostatic repulsion between electrical double layers of neighboring particles. But in the case of full neutralization by base as in previous works, electrostatic interactions were shielded by cations of base and electrostatic repulsion could almost be neglected. Also, an attractive force was generated from the mixing interaction of overlapping shell in aqueous solvent, since the distance between particle centers in the lattice-like microstructure decreased with increasing hydrophobicity of a shell polymer.

It is well known that the stability of sterically stabilized particles is significantly influenced by the solubility of polymers added to the suspension. An excess chemical potential which would arise in the overlap of the grafted polymer layers can cause steric repulsion between approaching particles.[11,12] The repulsion energy is dependent on the affinity of the grafted polymer layers for the dispersion medium. The steric stabilization theory has been extended by several investigators.[13,14]

In this article, the effects of hydrophobic interactions on the rheological behavior and microstructure of suspension of carboxylated core-shell latex particles with changing hydrophobicity of shell polymer and suspending medium are studied. These effects are discussed using the steric stabilization theory for grafted polymer layers on the surface of the particles.

Correspondence to: H. Nakamura (nakamura@mosk.tytlabs.co.jp).

TABLE I
Monomer Composition of the Core-Shell Particles

	Weight ratio			
	First stage (Core)	Second stage (Shell)		
		CS-1	CS-5	CS-6
MMA	47	24	16	6
n-BA	50	38	46	56
AMA	3			
MAA		18	18	18
HEA		20	20	20

EXPERIMENTAL

Preparation of suspensions of carboxylated core-shell particles

Carboxylated core-shell particles (CS-1, CS-5, and CS-6) were obtained by semicontinuous two-stage feed emulsion polymerization.[1,10,15,16] In all particles, core polymers were crosslinked and shell polymers were linear and grafted to the core. Monomer compositions are shown in Table I. The weight ratio of monomers of the core polymer/shell polymer was 100/29.5. Though the core composition of every particle was the same, the weights of *n*-butyl acrylate (*n*-BA) and methyl methacrylate (MMA) in the shell polymers were different. Weight ratios *n*-BA/MMA of CS-1, CS-5, and CS-6 were 38/24, 46/16, and 56/6, respectively. The hydrophobicity of these shell polymers was CS-1 < CS-5 < CS-6, because the hydrophobicity of *n*-BA is higher than that of MMA. The core diameter measured with dynamic light scattering equipment (Otsuka Electronics ELS-800, Osaka, Japan) in diluted suspension (0.1 wt %) was 90 nm. Diameters of CS-1, CS-5, and CS-6 were 180, 170, and 160 nm, respectively, with carboxyl groups fully neutralized by 2-dimethylaminoethanol (DMAE).

Suspensions of the carboxylated core-shell particles CS-6 were prepared with two suspending media, namely, water and a 9/1 (w/w) water/1-butanol mixture.

In every suspension, the concentration of the particles was 20 wt % and carboxyl groups of the particle were fully neutralized by DMAE.

Rheology measurements on suspensions

Steady shear rate viscosity η was measured with varying shear rate $\dot{\gamma}$ from 1×10^{-2} to 5×10^{2} s^{-1}. Every sample was subjected to a strain amplitude sweep at a set frequency to check the linearity of the measurements. Storage modulus G' and loss modulus G'' were measured with changing strain amplitude γ from 1×10^{-3} to 5×10^{1} % at an angular frequency of $\omega = 1 \times 10^{1}$rad s^{-1}. G' and G'' were measured with changing ω from 1×10^{-2} to 1×10^{2} rad s^{-1} in the linear γ region with a rotational type rheometer (Rheometrics ARES, New Jersey, USA) equipped with a conical-cylinder fixture.

Microstructures of suspensions of the core-shell particles were studied by small-angle X-ray scattering (SAXS) measurements. SAXS conditions have been described elsewhere.[10] An interparticle distance ξ (center to center distance) of the particles in the lattice-like structure was derived from the first peak position in the plot of the scattering vector Q versus X-ray intensity.

RESULTS AND DISCUSSION

Effects of hydrophobicity of shell polymer on microstructure

Figure 1 shows the steady shear rate viscosity η of suspensions of the core-shell particles plotted against shear rate $\dot{\gamma}$ for varying hydrophobicity of shell polymer. With increasing hydrophobicity, η and the degree of shear-thinning decreased. From our previous research, this behavior is known to be caused by deformation of the microstructure of the particles with increasing hydrophobicity of shell polymer.[1]

To clarify the change in the microstructure of the suspension, dynamic oscillatory rheological measurements and SAXS measurements were investigated. Figure 2 shows storage modulus G' and loss modulus G'' of the suspension plotted against strain amplitude γ. Above the critical amplitude, γ_{crit}, the response became nonlinear, causing the storage modulus (G') to

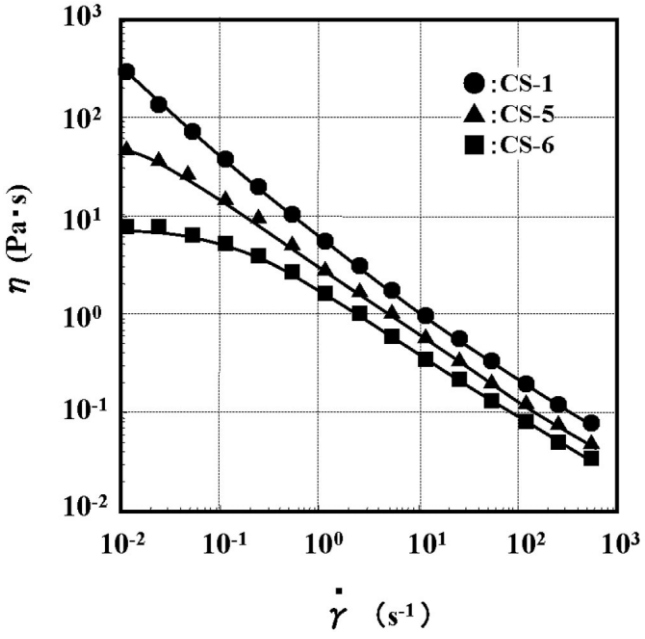

Figure 1 Steady shear rate viscosity η as a function of shear rate $\dot{\gamma}$ for various core-shell particles suspensions with different hydrophobicity of shell; ●:CS-1, ▲:CS-5, ■:CS-6.

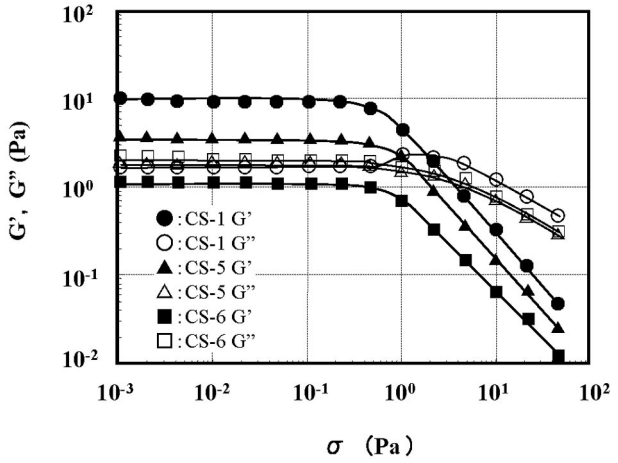

Figure 2 Dynamic storage modulus G' and loss modulus G'' as a function of strain γ for various core-shell particles suspensions with different hydrophobicity of shell; ●○:CS-1, ▲△:CS-5, ■□:CS-6.

decrease. All of these suspensions had nonlinear regions, and γ_{crit} and G'' were almost the same, but G' decreased with increasing hydrophobicity. This means that these suspensions displayed an elastic response caused by microstructures being disrupted by large stresses and that the strength of the microstructures decreased with increasing hydrophobicity of the shell polymer. Figure 3 shows G' and G'' of the suspension plotted against angular frequency ω. G' and G'' depended on ω in every case, but the slopes of G' and G'' decreased with increasing hydrophobicity. CS-1 indicated more pronounced viscoelastic behavior, with G' flattening out at high frequencies, and elastic solid-like behavior was observed. Here G' was high and almost independent of frequency. A characteristic frequency, ω_c, can be determined from where $G' = G''$ (tan $\delta = 1$). This is a very sensitive parameter and shows the transition from liquid-like (tan $\delta > 1$) to solid-like (tan $\delta < 1$) behavior. ω_c of CS-1, CS-5, and CS-6 were about 2×10^{-2}, 5×10^{-1}, and 2×10^{1}, respectively. As the suspension had three-dimensional network structure in the $\omega > \omega_c$ region and isolated structured domains below $\omega < \omega_c$,[17,18] the width of the ω region in which the suspension had three-dimensional network structure decreased with increasing hydrophobicity. These results indicated that the volume fraction of microstructures made up of the particles in the suspension decreased with increasing hydrophobicity of the shell polymer. SAXS profiles of the suspensions of CS-1, CS-5, and CS-6 are shown in Figure 4. In every case, a diffraction peak was detected. This means that these suspensions had lattice-like microstructures. The heights of the diffraction peaks were almost the same, however the peak angle of the SAXS curve decreased with increasing hydrophobicity. The interparticle distances ξ of CS-1, CS-5, and CS-6 were found to be 134,

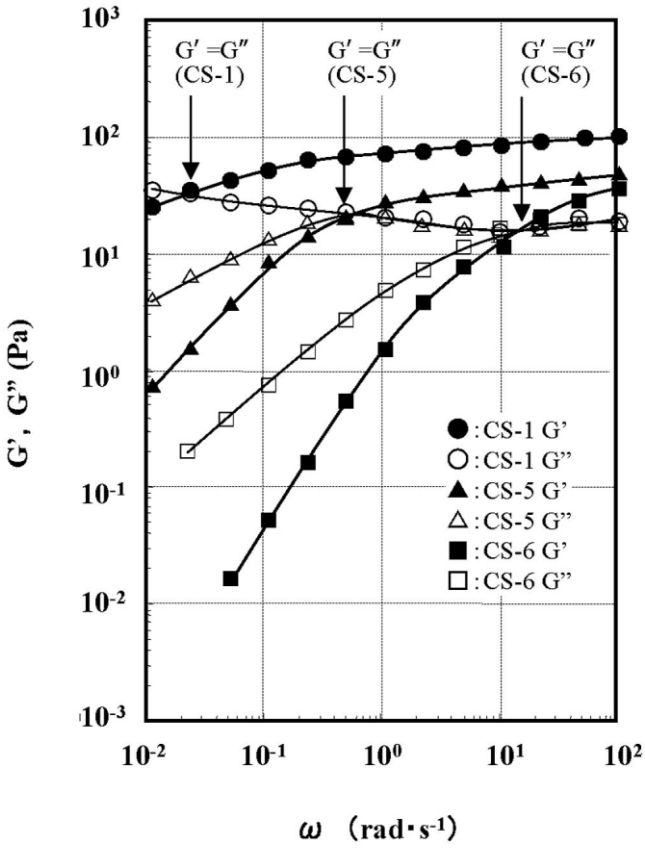

Figure 3 Dynamic storage modulus G' and loss modulus G'' as a function of angular frequency ω for various core-shell particles suspensions with different hydrophobicity of the shell; ●○:CS-1, ▲△:CS-5, ■□:CS-6.

128, and 124 nm, respectively, from the radial distribution function curves. These indicated that ξ increased with an increase in hydrophobicity of the shell polymer, though the number of particles in the structure remained almost constant. With increasing hydrophobicity of the particle, interparticle distance in the microstructure decreased, as did the volume of the microstructure (shown schematically in Fig. 5).

Effect of hydrophobicity of the suspended medium

Figure 6 shows G' and G'' of the water/1-butanol mixture suspension of CS-6 plotted against ω, com-

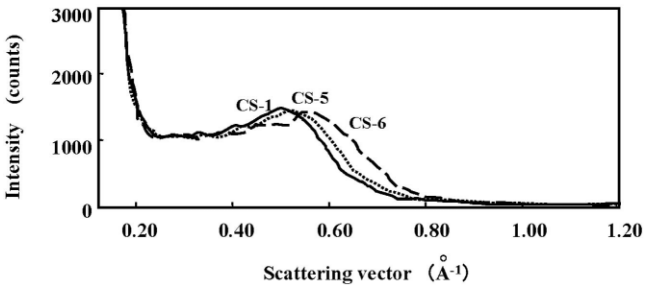

Figure 4 SAXS profiles of various suspensions of the core-shell particles with different hydrophobicity of shell; solid line: CS-1, dotted line: CS-5, broken line: CS-6.

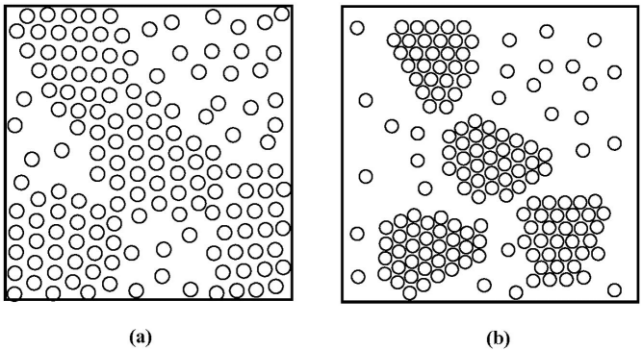

Figure 5 Schematic illustration of microstructures for core-shell particles suspensions with different hydrophobicity of the shell; (a) low hydrophobicity and (b) high hydrophobicity.

pared with that of an aqueous suspension. The slopes of G', G'', and ω_c decreased when the suspending medium changed from water to the water/1-butanol mixture. As G' and G'' of the water/1-butanol suspension were almost independent of ω, the microstructure changed from a collection of isolated structured regions to a three-dimensional network when changing

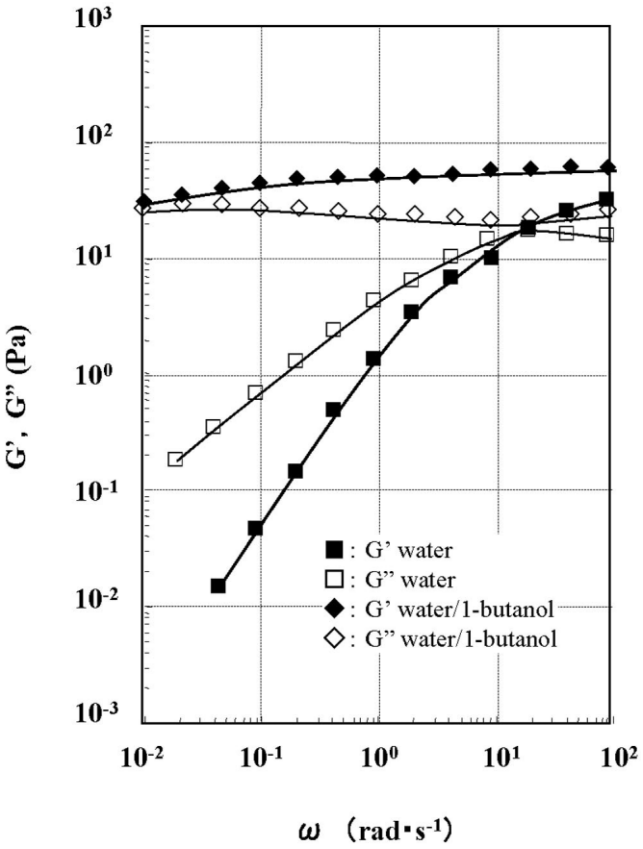

Figure 6 Dynamic storage modulus G' and loss modulus G'' as a function of angular frequency ω for the CS-6 suspensions with different suspending medium hydrophobicity; ■□:water, ◆◇:water/1-butanol mixture.

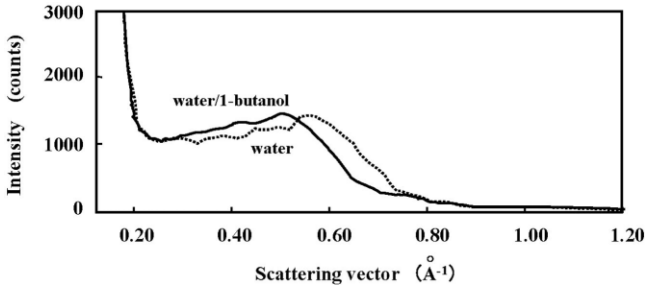

Figure 7 SAXS profiles of the CS-6 suspensions with different suspending medium hydrophobicity; dotted line: water, solid line: water/1-butanol.

the suspending medium from water to water/1-butanol. These results suggested that the volume fraction of the microstructure increased with increasing hydrophobicity of the suspending medium. A SAXS profile of the water/1-butanol suspension of CS-6 is compared with that of an aqueous suspension in Figure 7. The peak position of the SAXS curve was shifted to lower angle but the height of the diffraction peak was almost the same. These results indicated that ξ increased with change in medium from water to water/1-butanol, i.e., with increasing hydrophobicity of the suspended medium. But a number of the particle in the microstructure is almost the same.

Effect of hydrophobicity on the interaction between the particles

We approached the effect of the hydrophobicity of shell polymer and suspending medium on microstructure and rheological behavior from the point of view of the steric stabilization theory.

The diameter D_{core} of the core particle was 90 nm, and diameters $D_{core/shell}$ of the fully neutralized core-shell particles CS-1, CS-5, and CS-6 were 180, 170, and 160 nm, respectively, (that is, $D_{core} < \xi < D_{core/shell}$). Thus, shells of neighboring particles overlapped each other in the microstructure (Fig. 8). Effects of the shell polymer hydrophobicity on the microstructure are explained by a model of sterically stabilized particles with grafted polymer layers on their surfaces.

In this case, particle interaction occurs as soon as the grafted layers start to overlap. When two spheres (radius a) surrounded by a grafted layer (thickness δ) are forced to approach to a surface-to-surface distance h that is less than 2δ, then some overlap of the layers will occur, along with a reduction in chemical potential of the solvent in the overlap region and an increase in osmotic pressure (as a result of the increase in segment density) in the same region. As a result, solvent will diffuse from the bulk to the overlap region, separating the particles, i.e., leading to repulsion. The free energy, δ (G_{mix}), is given by the following expression,

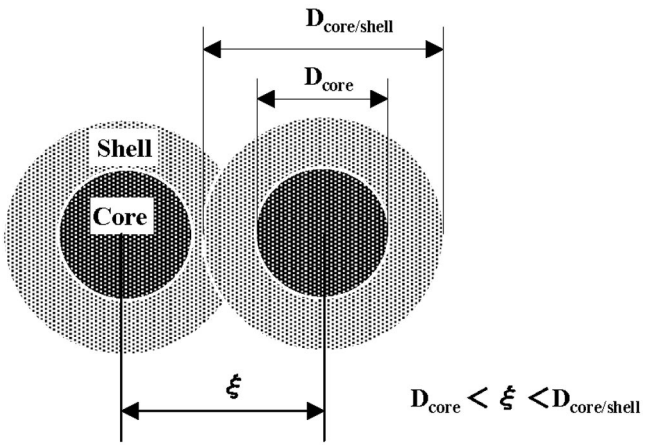

Figure 8 Schematic illustration of overlapped shell layers of neighboring core-shell particles in the microstructure.

$$G_{mix} = kT\, V_2^2\, V_1^{-1}\, v_2\, (0.5-x)(\delta - 0.5h)^2(3a+2\,\delta+0.5h)$$

where V_1 and V_2 are the molar volumes of the polymer and solvent, respectively, ν_2 is the number of chains per unit area, and χ is the chain-solvent interaction parameter.

Clearly G_{mix} can be positive or negative (i.e., repulsive or attractive) depending on the magnitude of χ. When the chains are in a good solvent, i.e., $\chi < 0.5$, then G_{mix} is positive, i.e., repulsion occurs as a results of polymer overlap. In other words, mixing of the chains in this case is unfavorable. In contrast, when $\chi > 0.5$, i.e., the chains are under poor solvent conditions (worse than θ solvent), G_{mix} is negative and mixing of the chains is favorable, i.e., the mixing interaction in this case is attractive.

In the case of the carboxylated core-shell particles, since water is a poor solvent for the shell polymer, an attractive force is generated between two overlapping particles. As the order of hydrophobicity was CS-1 < CS-5 < CS-6, the strength of the attractive force was CS-1 < CS-5 < CS-6 (Fig. 9). The steric stabilization theory can explain the decrease in ξ with increasing hydrophobicity of the shell polymer. As the number of particles in the microstructures was almost the same, the volume fraction of the microstructure in the suspension was CS-1 > CS-5 > CS-6.

The effect of the hydrophobicity of the suspending medium on the microstructure can also be explained by the steric stabilization theory. In the case of the carboxylated core-shell particles, since 1-butanol is a better solvent than water for the shell polymer, the attractive force decreased with changing the medium from water to water/1-butanol. As a result, ξ in the water/1-butanol suspension was larger than in the aqueous suspension (Fig. 10). As the number of particles in the microstructures of the water/1-butanol suspension was almost the same, the volume fraction of the microstructure in water/1-butanol increased with the increase in hydrophobicity of the suspending medium. These effects of hydrophobic interaction on ξ in the lattice-like microstructures are explained by the sterically stabilized particle model.

CONCLUSIONS

The effects of hydrophobic interactions on the rheological behavior and microstructure of suspension of carboxylated core-shell latex particles with changing hydrophobicity of shell polymer and suspending medium are studied. These effects are discussed in the context of the steric stabilization theory which deals with grafted polymer layers on the surface of each particle. Carboxylated core-shell latex particles form lattice-like microstructures in suspension with full neutralization of carboxyl groups. With increasing hydrophobicity of the shell polymer, the center-to-center distance ξ of the particles in the microstructure de-

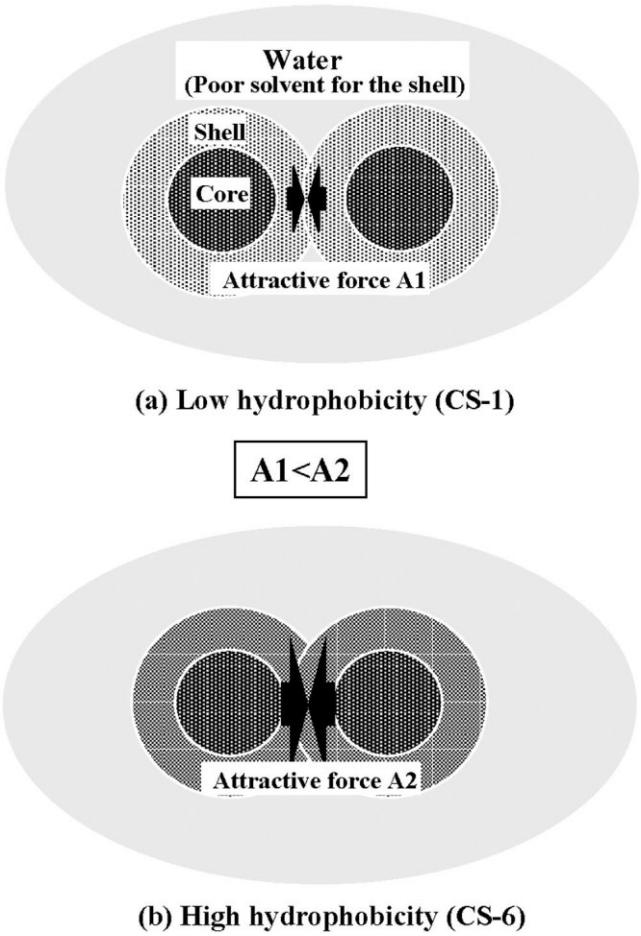

Figure 9 Schematic illustration of effect of shell hydrophobicity on microstructures of core-shell particle suspensions; (a) low hydrophobicity (CS-1) and attractive force A1, (b) high hydrophobicity (CS-6) and attractive force A2. The strength of attractive force is A1 A2.

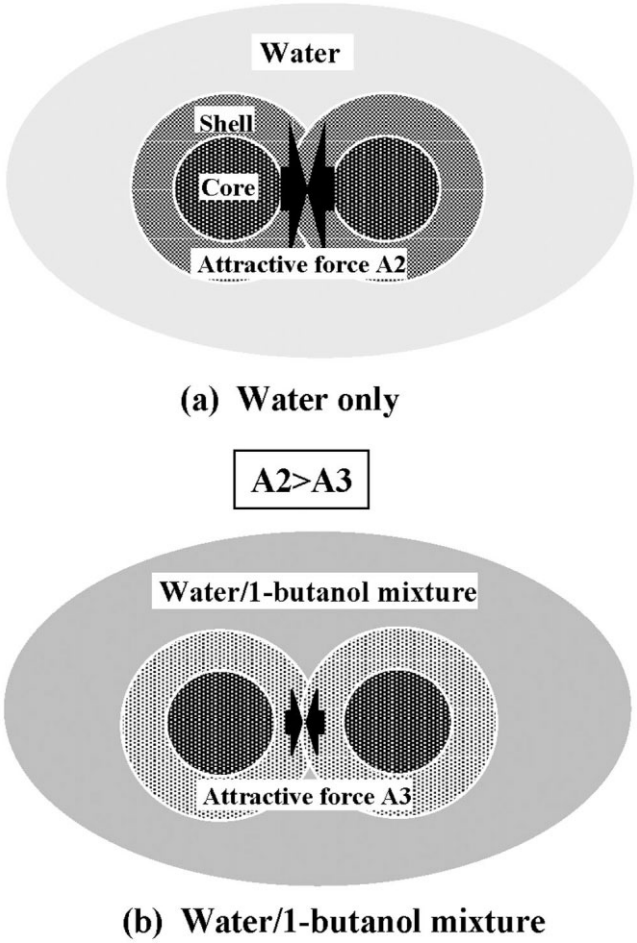

Figure 10 Schematic illustration of effect of suspending medium hydrophobicity on microstructures of suspensions of core-shell particles; (a) water only and attractive force A2, (b) water/1-butanol mixture and attractive force A3. The strength of attractive force is A2 A3.

creased. With increasing hydrophobicity of the suspending medium, ξ increased. The effect of hydrophobic interaction on ξ was explained by the steric stabilization theory for particles with grafted polymer on the surface. As the carboxylated core-shell latex particles overlapped each other in the microstructure, an attractive force was generated in the aqueous suspension between the particles. With increasing hydrophobicity of the shell, the attractive force increased. However, with increasing hydrophobicity of the suspending medium, the attractive force decreased.

References

1. Nakamura, H.; Tachi, K. J Appl Polym Sci 1996, 65, 1933.
2. Rowell, R. L. In An Introduction to Polymer Colloids; Candau, F., Ottewill, R. H., Eds.; Kluwer: The Netherlands, 1990; NATO ASI Series C, Vol. 303; Chapter 7.
3. Ford, J. R.; Morfesis, A. A.; Rowell, R. L. J Colloid Interface Sci 1985, 105, 516.
4. Snuparek, J.; Quadrat, O.; Horsky, J.; Kaska, M. L. In Polymer Colloids; Daniels, E. S., Sudol, E. D., El-Aasser M. S., Eds.; American Chemical Society: Washington, DC, 2002. ACS Symposium Series, Vol. 801; Chapter 6.
5. Quadrat, O.; Mrkvickova, L.; Snuparek, L. J Colloid Interface Sci 1988, 123, 353.
6. Bradna, P.; Stern, P.; Quadrat, O.; Snuparek, L. J Colloid Interface Sci 1995, 273, 324.
7. Van Beelen, D. C.; Metzger, C. W.; Buter, R.; Lichtenbelt, J. W. Th. In Proceedings of the 15th International Conference in Organic Coatings Science and Technology; 1989; p 39.
8. Vachlas, Z. J Oil Color Chem Assoc 1989, 77, 139.
9. Hoy, K. L. J Coat Technol 1979, 51, 27.
10. Nakamura, H.; Tachi, K. J Appl Polym Sci 2001, 79, 1627.
11. Fisher, E. W. Kolloid-Z 1958, 160, 120.
12. Ottewill, R.H., Walker, T. Kolloid-Z 1968, 227, 108.
13. Napper, D. H. Polymeric Stabilization of Colloidal Dispersions; Academic Press: New York, 1983.
14. Sato, T. Polymeric Stabilization of Colloidal Dispersions by Polymer Adsorption; Marcel Dekker: New York, 1980.
15. Kostansek, E. C. In An Introduction to Polymer Colloids; Candau, F., Ottewill, R. H., Eds.; Kluwer: The Netherlands, 1990. NATO ASI Series C, Vol. 303; Chapter 2.
16. Muroi, S.; Hashimoto, H.; Hosoi, K. J Appl Polym Sci 1984, 22, 1365.
17. Jones, D. A. R.; Leary, B.; Boger, D. V. J Colloid Interface Sci 1991, 147, 479.
18. Jones, D. A. R.; Leary, B.; Boger, D. V. J Colloid Interface Sci 1992, 150, 84.